



## Distribution of the iucD virulence gene among clinical *Escherichia coli* isolates in Iraq and evaluation of magnesium oxide nanoparticles as an antibacterial agent

Ishraq Abdulameer Salih<sup>1,\*</sup>, Abeer Fauzi Al-Rubaye<sup>2</sup>, Isra'a Qassim Mohsen Khalil<sup>3</sup>,  
Shaima Ahmed Rahim<sup>4</sup>, Raad A. Kadhim<sup>5</sup>

<sup>1</sup>University of Babylon. Department of biology. College of Science for Women, Babylon, Iraq.

\*Corresponding author: Ishraq Abdulameer Salih.

University of Babylon. Department of biology.  
College of Science for Women, Babylon, Iraq.

E-mail: asho2091@yahoo.com

DOI: <https://doi.org/10.54448/ijn26S206>

Received: 03-12-2026; Revised: 05-21-2026; Accepted: 06-08-2026; Published: 06-16-2026; IJN-id: e26S206

**Editor:** Dr Eemaz Nathaniel, MBBS.

### Abstract

*Escherichia coli* (*E. coli*) multidrug resistance is one of the most serious reasons for urinary tract and burn wound infections. In this context, the iucD virulence gene and the antibacterial and antibiofilm activity of magnesium oxide (MgO) nanoparticles were studied in 20 *E. coli* isolates from 50 Babylon patients in Iraq. High resistance to ampicillin and tetracycline, moderate susceptibility to ciprofloxacin and gentamicin, but full susceptibility to imipenem was shown by antimicrobial susceptibility testing. iucD gene was detected only in three (10%) isolates, representing a marked variability of virulence. The nanoparticles were analyzed by FE-SEM, XRD, FTIR and EDS techniques for spherical morphology of crystalline white particles well dispersed in the matrix. The nanoparticles showed concentration-dependent antibacterial activity with inhibition zones of 17 mm and 13 mm for 2 mg/mL and at 1 mg/mL, respectively, as well as significantly reducing the biofilm formation. These findings indicate that MgO nanoparticles can be used as a potential experimental antibacterial and antibiofilm therapeutic strategy against MDR and biofilm formers of *E. coli*. Although not aimed to the direct treatment of burn infections in humans, this study also fits into sustainable health research set forward towards UN Sustainable Development Goal 3 (Good Health and Well-being) as it represents an approach to seek novel strategies for fighting antimicrobial resistance or achieving better infection control.

**Keywords:** iucD gene. MgONPs. E.coli. UTI.

### Introduction

Nanotechnologies are rapidly developed, offering a novel approach to synthesize materials with desired properties for diverse applications. A significant emerging focus, which is receiving increasing attention, is the "green synthesis" of nanoparticles that utilizes biological organisms such as bacteria, fungi, or plants. This method is notably simple, environmentally friendly, and low-cost and generates biofriendly nanomaterials, in contrast to traditional techniques that are resourceconsuming, acidic, and thermal [1]. The reasons manganese oxide (MnO) nanoparticles are widely used are their magnetic, catalytic, and redox properties [2].

The growing worldwide public health threat of antimicrobial resistance (AMR) is one of the most pressing in the 21st century. The rampant abuse and misuse of traditional antibiotics has facilitated the emergence of multidrug-resistant (MDR) bacterial strains, with most antibiotics losing their potency against these life-threatening bugs. It is often the cause of serious and the most difficult-to-treat infections, such as burn and urinary tract infections, in which the capacity to form biofilms as well as to escape the immune system greatly complicates its treatment [3,4]. The bactericidal mode of action of MgO NPs is complex and mainly involves the formation

of ROS like the superoxide anions ( $O_2^-$ ) that impose oxidative stress and disturb bacterial structures, especially the membrane, proteins, and DNA [5].

Additionally, the physical contact of positively charged NPs with the negatively charged exterior wall of bacteria leads to the disruption of a membrane and release of intracellular material. The emergence of antimicrobial resistance in pathogenic bacteria at a worldwide level is currently one of the most serious threats to public health in the twenty-first century. Of these, *E. coli* is known to be an important pathogen responsible for community-acquired and nosocomial infections such as UTI, burn wound infection, and systemic diseases. Uropathogenic *E. coli* (UPEC) accounts for 70–90% of uncomplicated urinary tract infections (UTIs) around the world [6, 7]. Another relevant site of colonization is that the *E. coli* bacteria often occupies burn wounds and compromised tissues, where it also causes grave morbidity with heightened virulence and emerging resistance [7,8].

The most responsible cause for the pathogenicity of *E. coli* is a variety of virulence factors, such as adhesins, toxins, capsules, and iron-carrying systems. Iron Requirement: Iron is a necessary nutrient for bacterial survival and multiplication in the host, but it is tightly restricted by the host defense. Pathogenic strains produce siderophores such as aerobactin, which is encoded by the *iucABCD* operon to counteract this restrictive barrier. The *iucD* gene is a key factor in the creation of aerobactin, which promotes iron uptake and contributes greatly to bacterial virulence [9].

The *iucD* gene has been strongly linked to Extraintestinal Pathogenic *E. coli* (ExPEC), especially in the urinary tract and invasive infections [10]. With increasing antibiotic resistance to traditional antibiotics, nano-antimicrobial approaches have played a prominent role. The MgO NPs and zinc NPs have exhibited their efficacy as antibacterial agents in a broad spectrum because of the reactive oxygen species (ROS) generation, membrane damage, and the alkaline surface effect [11].

Its nanoparticles are promising candidates due to stability with relatively low toxicity and effectiveness against Gram-negative bacteria; hereupon, the body is to be considered as a potential alternative drug molecule for possible use at the nanoscale to control particle size-dependent bacterial activity. Therefore, the objective of the current study was to determine the prevalence of the *iucD* gene among *E. coli* strains isolated from urinary tract infections (UTI), burn infections, and other clinical sources in Iraq along with their susceptibility to magnesium oxide nanoparticle treatment.

## Materials and Methods

### Reporting Guidelines

This study was reported in accordance with the Strengthening the Reporting of Observational Studies in Epidemiology (STROBE) statement for prospective cohort studies.

### Chemicals and Reagents

All the chemicals, like  $MnSO_4$  and different culture media, were of analytical grade.

### Study Design and Clinical Samples collected

This research is a prospective cross-sectional analysis performed in the period from [4-4-2025] to [3-6-2025], in different hospitals in Hilah/Babylon, Iraq.

### Ethical Approval and Informed Consent

The study received ethical approval from the [College of Science of Women Ethics Committee]. Clinical specimens (twenty (20) (burn and UTI)) were obtained from [50] patients.

### Procedures and Samples

Burn wound samples were collected by sterile swabs, and urine samples were obtained midstream using a sterile container. Samples were all taken to the laboratory in a cool box and processed within two hours of collection.

### Bacterial Isolation and Culture

Clinical samples were cultured on routine culture media such as Blood agar, MacConkey agar and incubated at 37°C for 24 h. Common morphology features of bacterial colonies like the presence of  $\beta$ -hemolysis over the Blood Agar, non-lactose fermenting colonies over the MacConkey Agar was used to screen the presumptive *E. coli*. Colonies were subcultured on selective and differential media for further validation. One of the media used was chromog Agar. All the isolates were tested in viteck 2 system [7].

### Ast profile

Antimicrobial sensitivity testing was carried out by the disc diffusion method on Mueller–Hinton agar (HiMedia Lab., India) to standardize control of procedures as recommended in the Clinical and Laboratory Standards Institute (CLSI, current). The antibiotics tested mainly represented the most frequently used drugs in Iraqi hospitals (e.g., ampicillin, ciprofloxacin, cefotaxime, gentamicin, imipenem, etc.). Inhibition zones were measured and interpreted as susceptible, intermediate, or resistant

using CLSI breakpoints. The bacteria strains were purchased from standard culture collections as well as clinical isolates, and for bio-nanopreparation, *Bacillus subtilis* A pure culture of *B. subtilis* was preserved on nutrient agar (NA) slants at 4°C. For the synthesis of nanoparticles, a single colony was transferred to 100 mL of nutrient broth (NB) (Himedia, India), and the culture was incubated at 37°C in a rotary incubator (150 rpm) for 24 hours [12].

### Bio Synthesis of MnO Nanoparticles

The cell-free supernatant of *Bacillus subtilis* culture was used for synthesis. The cells were separated by centrifugation after 24 h of culture. The supernatant obtained thereby was combined with 0.1 M manganese sulfate. After the assistance of 60°C to form MgO-oxides, the reaction solution was adjusted to pH by adding NaOH (or 8.0 strontium hydroxide) in order to produce MgO, which was visually identified by the brown precipitate that started to precipitate. then collected, and the nanoparticles were washed and freeze-dried for further characterization and applications [2].

### Chemical Characterization

The produced MnO nanostructure was characterized by several techniques to verify the reported property. UV-VIS spectroscopy confirmed nanoparticle formation. X-ray Diffraction (XRD) was used to analyze the crystal structure and size. The morphology and size of particles were characterized with a Scanning Electron Microscopy (SEM) and a Transmission Electron Microscopy (TEM), and the functional groups of the biological supernatant responsible for the capping of these nanoparticles were confirmed by Fourier Transform Infrared Spectroscopy (FT-IR) [2].

### Antibacterial Effect

Antibacterial Testing: The antibacterial ability of the nanoparticles against the clinical strain of *E. coli* was evaluated by the conventional agar diffusion technique on the agar plates of Mueller-Hinton, according to the mid-2015 protocol [13].

### Minimum inhibition concentration (MIC test)

An antimicrobial sensitivity test for *E. coli* was done according to the KirbyBauer disk diffusion method according to CLSI to have a turbidity equal to 0.5 McFarland standard (approximately 1.5×10<sup>8</sup> CFU/mL). A fresh overnight culture of *E. coli* was tested. And after that, a sterile cotton swab was used to evenly spread the bacterial inocula on Mueller-Hinton agar

plates. Disks from antibiotic panels (one variety) were placed on top of the agar after drying, and plates were maintained at 35°C for 16 to 18 hours. The inhibition zone of each disc is measured in mm [5].

### Biofilm and antibiofilm

The anticatheter biofilm formation potential of MgO-nanoparticles (MgO-NPs) was investigated using the crystal violet microtiter plate method against twenty clinical isolates of *E. coli* as described earlier with slight modifications. In brief, each isolate was grown overnight in 5 mL of TSB at 37°C, and the bacterial suspension was adjusted to a 0.5 McFarland (~1.5×10<sup>8</sup> cells/mL) and seeded in a 96-well flat-bottom polystyrene microplate. Different amounts of MgO nanoparticles were supplemented to the wells and measured based on the response to the side-dependent effective dose of biofilm formation. After an additional 24-h static incubation at 37°C, the free-floating cells were aseptically removed, and the adhered biofilms were rinsed once with sterile PBS. The remaining biomass was fixed with methanol, stained with 0.1% crystal violet solution for 15 mins, washed again, and then solubilized with 33% acetic acid. The absorbance at 595 nm was measured in a microplate reader, and the percentage of biofilm inhibition was determined when compared with nanoparticle-free control [14].

### Molecular technique

To identify the genetic cause of the antibiotic-resistant phenotype of the *E. coli* clinical isolates, the *iucD* gene was tested. Genomic DNA was prepared from the isolates by a commercial DNA extraction kit (Favorgen, Korea). The gene probe was amplified using specific primers [1]. PCR was carried out in standard conditions with amplicons of target gene fragments (Tables 1 and 2).

Table 1. primer sequence of *iucD* genes

Gene	Primer sequence (5-3)		Product size (bp)	Source
	Forward	Reverse		
<i>iucD</i>	ACAAAAAGTTCTA TCGCTTCC	CCTGATCCAGAT GATGCTC	714	Nisreen kaddim radi and al marzoqi 2023

Source: Own authorship.

Table 2 PCR condition of the gene used in current study.

Genes	Temperature ( c ) / Time					Cycle number
	Initial	Cycling condition			Final	
	Denaturation	Denaturation	Annealing	Extension	extension	
<i>iucD</i>	94 C°/5min	94C°/30 sec	58 C°/45 sec	72C°/30 sec	72C°/5min	30

Source: Own authorship.

## Statistical analysis

Experiments were repeated in triplicate. The results are presented as the mean  $\pm$  SD and were compared by one-way analysis of variance (ANOVA) and  $p < 0.05$  was considered statistically significant [15].

## Results

Among twenty clinical isolates from patients with UTI and burn in *Escherichia coli* was the most prevalent pathogen. The frequency of MDR isolates was high. The virulence-associated genes associated with adhesion and biofilm formation were affirmed by molecular characterization in the iucD-UTI isolates. Moreover this suggested a potential new alternative therapeutic strategy, and MgO nanoparticles had significant antimicrobial activity against MDR *E. coli* isolates. Statistical analyses further demonstrated significant differences ( $p < 0.05$ ) between treated and control groups. The results are shown here in the order of experimental design (Figure 1)

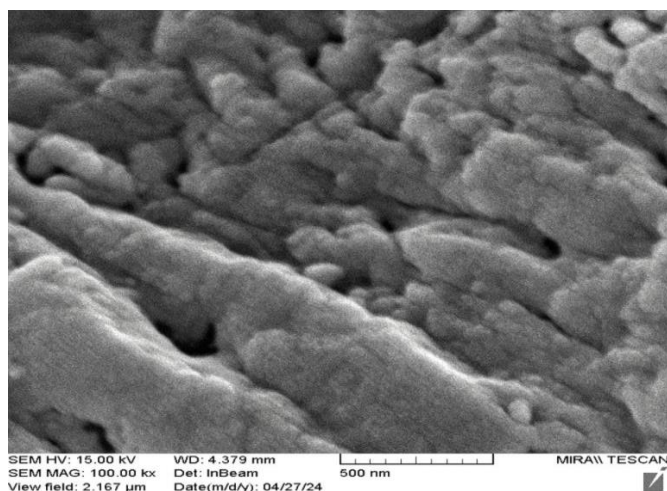


Figure 1. Field Emission Scanning Electron Microscopy (FESEM) images of synthesized Magnesium oxide (MgO) nanoparticles. The summary micrograph reveals more or less spherical particle shapes with weak bonding and a fairly homogenous orientation within the matrix. The particle size and surface morphology construction at the nanometer scale demonstrate that the NPs are prepared successfully. Source: Own authorship.

## X-ray diffraction (XRD)

The crystalline structure of MgO NPs. The XRD pattern showed diffraction peaks at  $2\theta = 17^\circ$ ,  $21^\circ$ , and  $31^\circ$ , which were attributed to the crystalline planes of the periclase phase of MgO. From these distinct peaks, the high crystallinity could be established with low amorphous content. The average nanoparticle size was calculated by the Debye–Scherrer equation, which evidenced the nanoscale dimension of halide

perovskite nanoparticles achieved here. These XRD results are in agreement with reported studies, indicating the successful formation of MgO nanoparticles for antibacterial applications (Figure 2).

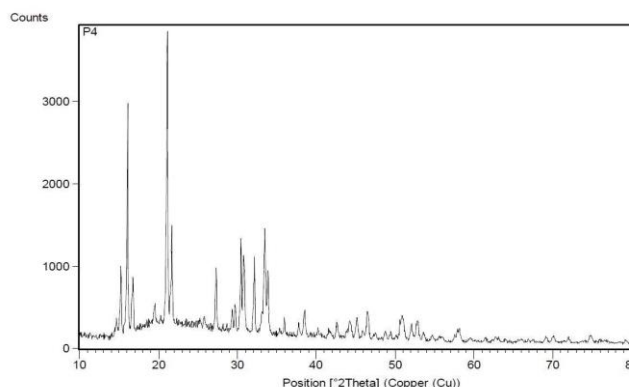


Figure 2. X-ray diffraction (XRD) pattern of synthesized MgO nanoparticles. The reflection peaks at  $2\theta$  values of  $17^\circ$ ,  $21^\circ$ , and  $31^\circ$  prove the crystal quality of MgO and reveal that a periclase phase structure is prepared. The sharp, recognizable peaks represent the high crystallinity and phase purity of the nanoparticles. Source: Own authorship.

## Fourier infrared transform analysis of MgO NPS

The FTIR was employed to confirm the chemical composition and the functional groups of MgO nanoparticles. The FT-IR spectrum showed a strong absorption band at about  $500\text{--}600\text{ cm}^{-1}$  related to Mg–O stretching vibration, which verifies the presence of magnesium oxide. The broad absorption bands at around  $3271\text{ cm}^{-1}$  and  $1659\text{ cm}^{-1}$  were assigned to the O–H stretching and bending vibrations of adsorbed water molecules on the surface of the nanoparticle. Other weak peaks around

$1441\text{--}1546\text{ cm}^{-1}$  may correspond to the residual carbonate groups, which might originate from the adsorption of atmospheric  $\text{CO}_2$ . Comparatively broader peaks represent the success of the synthesis of MgO NPs without an impure metal oxide composition and surface hydroxyl groups for the possible increase in antimicrobial effects (Figure 3 and Table 3).

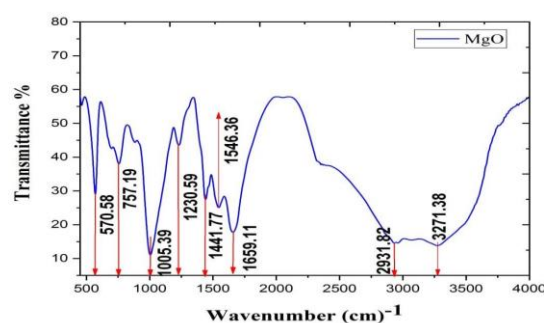


Figure 3. FTIR spectra of the as-prepared magnesium oxide (MgO) nanoparticles. The characteristic absorption band at  $500\text{--}600\text{ cm}^{-1}$  is attributed to the Mg–O stretching vibrations, which indicates that the MgO was formed. Corresponding broadband absorption at ca.  $3271\text{ cm}^{-1}$  and

1659 cm<sup>-1</sup> is assigned to the O–H stretching vibration mode of adsorbed water molecules and its bending, respectively, combined with a weaker band near 1441–1556 cm<sup>-1</sup>, suggesting some carbonate undertone contamination. Source: Own authorship.

Table 3. FTIR peak.

Peak Number	X (cm <sup>-1</sup> )	Y (%T)
1	3271.38	13.84
2	3063.42	15.49
3	2931.82	14.6
4	1659.11	17.77
5	1546.36	25.1
6	1441.77	27.49
7	1230.59	43.56
8	1005.39	11.07
9	757.19	38.05
10	570.58	29.02
11	463.17	55.34

Source: Own authorship.

### EDS Test

The EDS analysis on the MgO nanoparticles in the matrix indicated magnesium content at about 13.13 wt% and other elements such as carbon, nitrogen, oxygen, aluminum, silicon, phosphorus, potassium, and calcium in different amounts. Some of these factors could come from salts or filtration reagents in nanoparticle synthesis or the matrix itself. The MgNPs are crystalline, well dispersed, and chemically incorporated in the matrix, which is further supported by FESEM, XRD, and FTIR results (Figure 4 and Table 4).

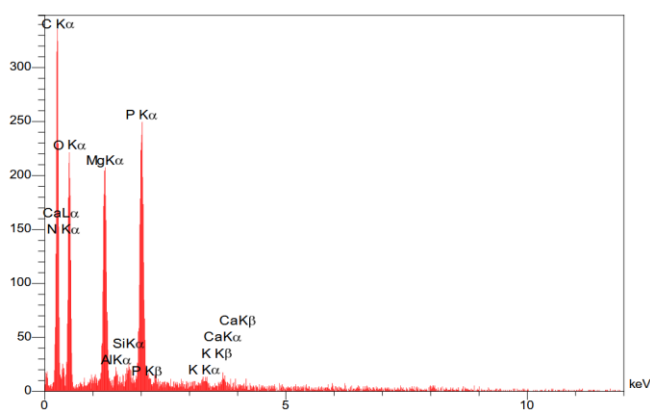


Figure 4. Energy Dispersive X-ray Spectroscopy (EDS) of the Prepared MgO NPs. The spectrum indicates the presence of Mg (13 wt%) and O as dominant constituents, with other elements such as C, N, Al, Si, P, K, and Ca. The presence of these minor elements could be associated with precursor salts, unreacted reagents, or environmental contamination during the sample preparation. Source: Own authorship.

Table 4. Elemental Analytical Results of MgO Nanoparticles by EDS Quantification.

Element	W%	A%
C	39.6	53.08
N	3.88	4.46

O	23.11	23.25
Mg	13.18	8.73
Al	0.47	0.28
Si	0.85	0.49
P	17.91	9.31
K	0.46	0.19
Ca	0.53	0.21

Source: Own authorship.

### Antimicrobial susceptibility test profile

The *E. coli* strains showed a variable pattern of resistance to the agents tested in the 20 isolates that were subjected to antimicrobial susceptibility testing. The greatest resistance emerged against ampicillin (90% of the isolates), and following close was tetracycline with 80%, as reports showed a generalized pattern of resistance to widely administered first-line drugs. Intermediate susceptibility was noted for ciprofloxacin (60% susceptibility) and gentamicin (70% susceptibility), while all isolates were found to be susceptible to imipenem, indicating the preservation of carbapenem activity against these strains. These results demonstrate that MDR-*E. coli* are prevalent in the study subjects, and continuous monitoring of antibiotic susceptibility patterns is essential, as well as considering the use of alternative antibacterial agents such as magnesium oxide nanoparticles. The rates of resistance profile and susceptibility among the isolates are presented in the chart (Figure 5).

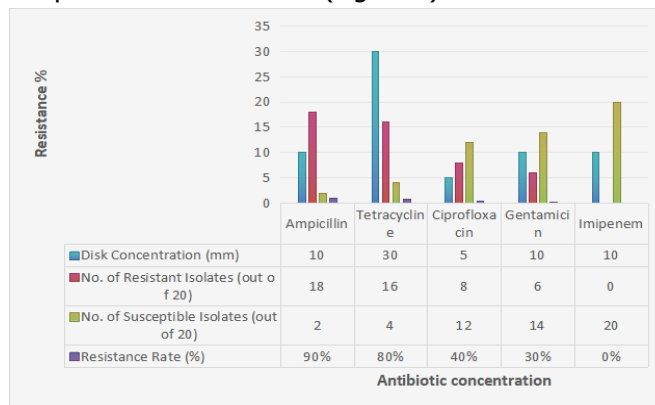


Figure 5. Antibiotic susceptibility test against *E. coli*. Source: Own authorship.

### Genetic Results

Out of twenty isolates of the clinical isolates, only two were positive for the iucD gene. Investigation at the molecular level indicated the presence of virulence-related gene(s) in these strains, suggesting their involvement in adhesion and persistence. PCR products of the target gene were detected with bands indicative of the expected size for base pairs in the PCR products, and thus successful capture. These results indicate that *E. coli* associated with IUCD strains might harbor distinct genetic determinants, which could be involved in colonization and infection. The PCR products were

analyzed on an electrophoresis gel (Figure 6).

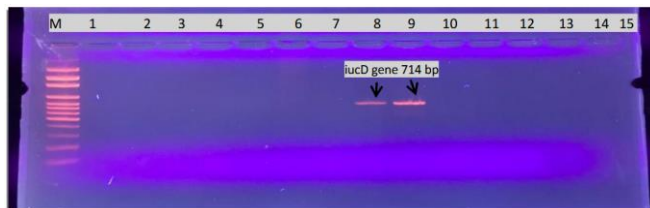


Figure 6. Gel Electrophoresis Pattern of iucD Amplicon 714 bp, among *E. coli* Isolated from Patient (1.5% Agarose at 75 Volts for 45 min) Line M: DNA ladder (100 bp); Lines 8, 9, and 1: positive results of amplification. Lines 1–7 and 10–15: negative results of amplification. Source: Own authorship.

### Antibacterial test

The antibacterial activity of magnesium oxide (MgO) NPs against *E. coli* isolates was determined by the agar well diffusion method at various concentrations. The nanoparticles showed concentration-dependent inhibition and a maximum at 2 mg/mL with a 17.0 mm zone of inhibition. At 1 mg/mL, the zone of inhibition was measured as 13 mm, and lesser concentrations (0.5 mg/mL and 0.25 mg/mL) did not present observable antibacterial effects (0 mm). These observations suggest that the bactericidal property of MgO nanoparticles increases with an increase in their concentration, as already reported for metal oxide nanomaterials (Figure 7).

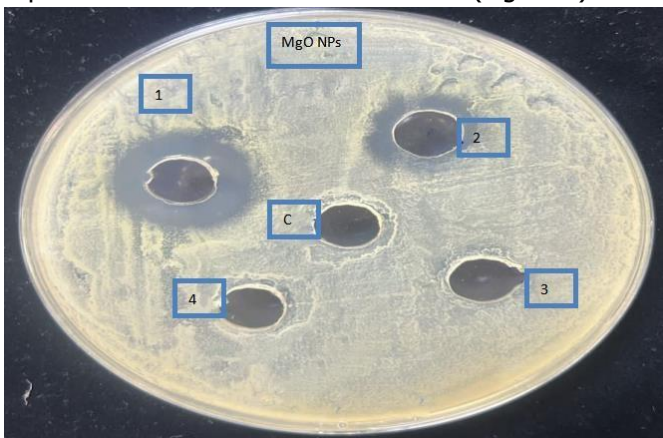


Figure 7. Antibacterial activity of MgO NPs against *E. coli* isolates at different concentrations. Source: Own authorship.

The inhibition zones (mm) were 17 mm for 2 mg/mL MgO, 13 mm for 1 mg/mL MgO, and no inhibition zone with the application of 0.5 mg/mL and a decline to as little as zero when an amount of 0.25 was reached, clearly indicating a concentration-based antibacterial impact, and C represented the control, distal water only.

### Biofilm and antibiofilm

Table 5 revealed the antibacterial activity of magnesium oxide (MgO) nanoparticles on *Escherichia coli* biofilm. The biofilm biomass was measured by

microtiter plate crystal violet assay. They indicate that the MgO-NPs exhibit concentration-dependent anti-biofilm activity, where higher concentrations strongly prevent biofilm formation as compared to the untreated control (Figure 8).

Table 5. Biofilm and antibiofilm bacterial activity of MgO nanoparticles.

Mean ± Std. Deviation	Biofilm formation by Pseudomonas		P value (P ≤ 0.05)
	Biofilm	Anti-Biofilm	
	0.2165±0.050	0.1206±0.023	0.00059*

\*Significant difference under  $p \leq 0.05$  by T-test.

Source: Own authorship.

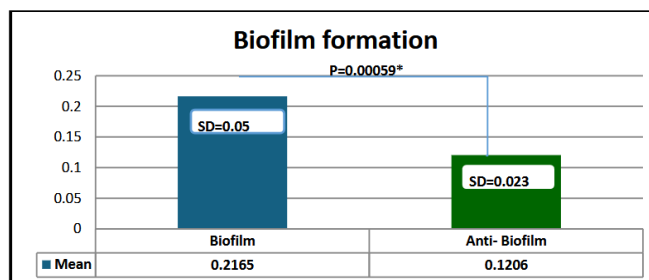


Figure 8. Biofilm and anti-biofilm activity detection by MgO NPs against *E. coli* isolates. Source: Own authorship.

### Discussion

In view of the steadily increasing MDR issue, alternative treatment modalities are urgently needed. Antimicrobials based on nanotechnology, especially the metal and metal oxide nanoparticles, have shown good antibacterial/antibiofilm activity via membrane damage, generation of ROS nanotechnology, ROS, and interference with intracellular functions [16]. These approaches may provide potential adjunct or alternative options to fight MDR *E. coli* isolates related to iucD-induced UTIs and burn wound infections.

In the current study, *Escherichia coli* was found to be a common pathogen among twenty clinical isolates obtained respectively from UTI and burn patients. Molecular characterization confirmed the presence of virulence-related genes in some isolates, suggesting their pathogenicity. MDR phenotypes detected in these isolates are similar to Iraqi studies ROS, studies, which have reported high percentages of ESBL-producing and MDR *E. coli* among UTI cases [7,8,17,18].

The characterization of MgO nanoparticles, suggested as a potential antibacterial material, was confirmed for their applications in the field of biomedical engineering. FESEM characterization revealed mostly spherical nanoparticles with agglomeration that was relatively weak and dispersed evenly in the matrix (Figure 1). The XRD patterns demonstrated well-defined peaks at  $2\theta$  angles of  $17^\circ$ ,

20°, and 31°, indicating that a crystalline phase, periclase, was synthesized with high purity (Figure 2). FTIR spectroscopy showed characteristic MgO stretching vibrations at 500–600 cm<sup>-1</sup> and broad O–H bands at -3271 and 1659 cm<sup>-1</sup>, whereas EDS confirmed the elemental composition (Mg -13 wt% and other elements C, N, O, Al, Si, P, K, and Ca) as of the salts employed during synthesis or in the matrix (Figures 3 and 4).

The findings of these results reveal that the MgO nanoparticles were crystalline, distributed homogeneously, and chemically integrated, which could be attributed to their structural and chemical characteristics for observed antibacterial and antibiofilm activity [1,19,20]. Antimicrobial susceptibility testing showed high resistance to ampicillin (90%) and tetracycline (80%), moderate sensitivity to ciprofloxacin (60%) and gentamicin (70%), and complete susceptibility to imipenem. These data cohere with studies describing the emergence of MDR *E. coli* in hospital and community populations [6,21,22]. The fact that the resistance rate to routine antibiotics is unacceptably high emphasizes the requirement for alternative therapeutic approaches (Figure 5).

On the other hand, the *iucD* gene, an important virulence factor that is responsible for aerobactin-mediated iron acquisition and virulence in ExPEC (1), was found in only 2/20 (10%) of our isolates when screened by a molecular method (Figure 6). This low prevalence implies that the majority of clinical infections in this group are due to strains without this virulence determinant. The presence of *iucD* in a portion of isolates could provide these with improved virulence potential, especially under conditions of iron limitation, as has been reported for other regions [7,9,10,22-24].

MgO NPs and ZnONPs have displayed strong antibacterial activity against *E. coli*, mainly due to ROS production and membrane destruction as well as cellular disintegration, suggesting that these nanoparticles will be potential agents for treatment of MDR and biofilm infections [5,16]. Thus, incorporation of nanotechnology-based strategies like MgO nanoparticles could potentially serve as an alternative to combat resistance and medical device-related infections (Figure 7).

In summary, the combination of nanoparticle characterization, phenotypic resistance profiling, biofilm formation, and genetic screening highlights a diverse pathogenicity profile in *E. coli*. The crystal and well-dispersed MgO-NPs exhibited potential antibacterial/antibiofilm activity that encouraged them to be used as alternative or synergistic agents in the

treatment of MDRE *E. coli* biofilm. These observations also underscore the value of ongoing molecular monitoring for virulence marker genes (e.g., *iucD*) to guide directed infection control interventions in Iraq and comparable clinical environments [25,26].

## Conclusion

Nanoscale magnesium oxide (MgO) was prepared, and its antibacterial/antibiofilm activities were applied against uropathogenic and burn isolates of multidrug-resistant *Escherichia coli* in Babylon, Iraq. Characterization proved that the nanoparticles were crystalline, highly dispersed, and chemically stable. In contrast, a very limited number of isolates were positive for the *iucD* virulence gene, indicating that strain pathogenicity was heterogeneous. While the MgO NPs showed potential *in vitro* activity, they are not intended for the human treatment of burn infections. However, additional studies are required to evaluate their safety, effectiveness, and deliverability, emphasizing their role as a research tool for targeting resistant and biofilm bacteria. AST profile antimicrobial sensitivity testing was carried out by the disc diffusion method on Mueller–Hinton agar (Hi-Media Lab., India) to standardize control of procedures as recommended in the Clinical and Laboratory Standards Institute (CLSI, current). The antibiotics tested mainly represented the most frequently used drugs in Iraqi hospitals (e.g., ampicillin, ciprofloxacin, cefotaxime, gentamicin, imipenem, etc.). Inhibition zones were measured and interpreted as susceptible, intermediate, or resistant using.

## CRedit

**Author contributions:** Salih and Al-Rubaye : Methodology, Project Administration. Khalil; Rahim; and Kadhim : Review & Editing.

## Acknowledgment

The authors wish to express their gratitude to all individuals and institutions that provided support during the course of this study. Special thanks are extended to those who contributed to the study design, data collection, and analysis.

## Ethical Approval

This study was performed in accordance with the Declaration of Helsinki and was reviewed and approved by the Ethics Committee of [College of Science for Women of University of Babylon] (approval no. [75] in 19-3-2026). All participants (or their legal guardians) provided written informed consent before the *E. coli* clinical isolates were collected. Data were anonymized

to protect patient confidentiality.

### Informed Consent

Informed consent was obtained from all participants involved in the study, with all procedures explained in detail before participation.

### Funding

Not applicable.

### Data Sharing Statement

The datasets used and analyzed during the current study are available from the corresponding author on reasonable request, and all data is stored following privacy and ethical guidelines

### Conflict of Interest

The authors declare no conflict of interest.

### Similarity Check

It was applied by Ithenticate®.

### Application of Artificial Intelligence (AI)

Not applicable.

### Peer Review Process

It was performed.

### About The License©

The author(s) 2026. The text of this article is open access and licensed under a Creative Commons Attribution 4.0 International License.

### References

1. Abinaya S, HP Kavitha M. Prakash, and A. Muthukrishnaraj, Green synthesis of magnesium oxide nanoparticles and its applications: A review. *Sustainable Chemistry and Pharmacy*, 2021, 19: 100368.
2. El-Zahed AAZ, ME Khalifa, MM El-Zahed, ZA Baka. Biological synthesis and characterization of antibacterial manganese oxide nanoparticles using *Bacillus subtilis* ATCC6633. *Scientific Journal for Damietta Faculty of Science*, 2023, 13(3): 79-87.
3. Kadhim HJ, NK Radi, SJ AL-Zuwaini, AH Almarzoqi, A Al-Nafiey IA, Ibraheem HA, Ali HW, Al-Kaim FF. Abd Alsada, H.M. Anber, and N.M. Obaid, Antibacterial and anticancer activity of new nanocomposite against *Acinetobacter baumannii*. *Microbial Biosystems*, 2025, 10(4): 164-178.
4. Prestinaci F, P Pezzotti, A Pantosti. Antimicrobial resistance: a global multifaceted phenomenon. *Pathogens and Global Health*, 2015, 109(7): 309318.
5. Radi NK, HA Mohammed, RJ Alwarid, RJ Alwarid, NA Mohammed, RMJ Ewadh. Polyvinylpyrrolidone-loaded Zn and ZnO nanoparticles influence *Escherichia coli* isolated from urinary tract infection patients. *Pharmakeftiki*, 2025, 37(2S).
6. Ho CS, et al., Antimicrobial resistance: a concise update. *Lancet Microbe*, 2025, 6(1): 100947.
7. Radi NK, AH Al-Marzoqi. The distribution of antimicrobial resistance and the presence of virulence genes in *Escherichia coli* isolated from frozen chicken meat in Iraq. *AIP Conference Proceedings*, 2023, 2776(1).
8. Maitz JJ, Merlino S, Rizzo G, McKew, P Maitz. Burn wound infections microbiome and novel approaches using therapeutic microorganisms in burn wound infection control. *Advanced Drug Delivery Reviews*, 2023, 196: 114769.
9. Herrero MV, de Lorenzo, JB Neilands. Nucleotide sequence of the *iucD* gene of the pColV-K30 aerobactin operon and topology of its product studied with *phoA* and *lacZ* gene fusions. *Journal of bacteriology*, 1988, 170(1): 56-64.
10. Mojaz-Dalfardi N, D Kalantar-Neyestanaki, Z Hashemizadeh, S Mansouri. Comparison of virulence genes and phylogenetic groups of *Escherichia coli* isolates from urinary tract infections and normal fecal flora. *Gene Reports*, 2020, 20: 100709.
11. Almontasser AA, Parveen, A Azam. Synthesis, Characterization and antibacterial activity of Magnesium Oxide (MgO) nanoparticles. *IOP Conference Series: Materials Science and Engineering*, 2019, 577(1): 012051.
12. Kaddim Radi N, R Issam AL-Daher, H Jawad Kadhim. A Novel Antibacterial and Anticancer Property of Iraqi Honey Bee Venom. *International Research Journal of Multidisciplinary Scope*, 2025.
13. Radi N, R Al-Daher, H Kadhim. A Novel Antibacterial and Anticancer Property of Iraqi Honey Bee Venom, 2025.
14. Albejawy HHAA, NK Radi, ME. Al-Defiery, Gene expression modulation of *brpA* gene in *streptococcus mutans* by zinc/bee venom/chitosan nano composites. *AIP Conference Proceedings*, 2025, 3395(1).
15. Vaux DL, F Fidler, G Cumming. Replicates and repeats—what is the difference and is it

- significant? The EMBO Reports, 2012, 13(4): 291-296.
16. Hajipour MJ, KM. Fromm, A.A. Ashkarran, D. Jimenez de Aberasturi, I.R. de Larramendi, T. Rojo, V. Serpooshan, W.J. Parak, and M. Mahmoudi, Antibacterial properties of nanoparticles. Trends Biotechnol, 2012, 30(10): 499-511
  17. Meshach F. Green synthesis, characterization and applications of manganese oxide nanoparticles. NanoEra, 2025, 5(1): 28-41.
  18. Somily AM, MZ Arshad, GA. Garaween, and A.C. Senok, Phenotypic and genotypic characterization of extended-spectrum  $\beta$ -lactamases producing *Escherichia coli* and *Klebsiella pneumoniae* in a tertiary care hospital in Riyadh, Saudi Arabia. Ann Saudi Med, 2015, 35(6): 435-439.
  19. Velho-Pereira S, MV Parmekar. Synthesis and Antibacterial Properties of Manganese Dioxide Nanostructures: A Review. ChemistrySelect, 2024, 9(38): e202402247.
  20. Krishnamoorthy K, G Manivannan, SJ Kim, K Jeyasubramanian, M Premanathan. Antibacterial activity of MgO nanoparticles based on lipid peroxidation by oxygen vacancy. Journal of Nanoparticle Research, 2012, 14(9): 1063.
  21. Yarob A, Z Sharba, S Abdulsahib. Investigation of Antibiotic Resistance Genes in *E. coli* Isolates from Patients in Iraq, 2024.
  22. Johnson JR, TA. Russo, Molecular Epidemiology of Extraintestinal Pathogenic *Escherichia coli*. EcoSal Plus, 2004, 1(1): 10.1128/ecosalplus.1128.1126.1121.1124.
  23. Mohammed EJ, KC Hasan, M Allami. Phylogenetic groups, serogroups and virulence factors of uropathogenic *Escherichia coli* isolated from patients with urinary tract infection in Baghdad, Iraq. Iran J Microbiol, 2022, 14(4): 445-457.
  24. Adnan I, A Saleh, H Kadhim, Z Al-Mahdi, A Al-Mahdi. Short Communication Molecular diagnostic of *Escherichia coli* among urinary tract infections' patients using polymerase chain reaction (PCR). Pakistan Journal of Biotechnology, 2016, 13: 275-278.
  25. Elmi SYK, MS Ashour, FZ Alsewy, NF. Abd El Moez Azzam, Phenotypic and genotypic detection of extended spectrum  $\beta$ -lactamases among *Escherichia coli* and *Klebsiella pneumoniae* isolates from type 2 diabetic patients with urinary tract infections. African health sciences, 2021, 21(2): 497-504.
  26. Neves FE de F, Pagioro YF, Castro FPL de. Major clinical outcomes of the endodontic infections and gut microbiota axis: a systematic review. MedNEXT J Med Health Sci [Internet]. 2025 Jan. 23 [cited 2026 Jun. 16];6(1). Available from: <https://mednext.zotarellifiloscientificworks.com/index.php/mednext/article/view/416>